Environment Canada Environnement Canada

Canada

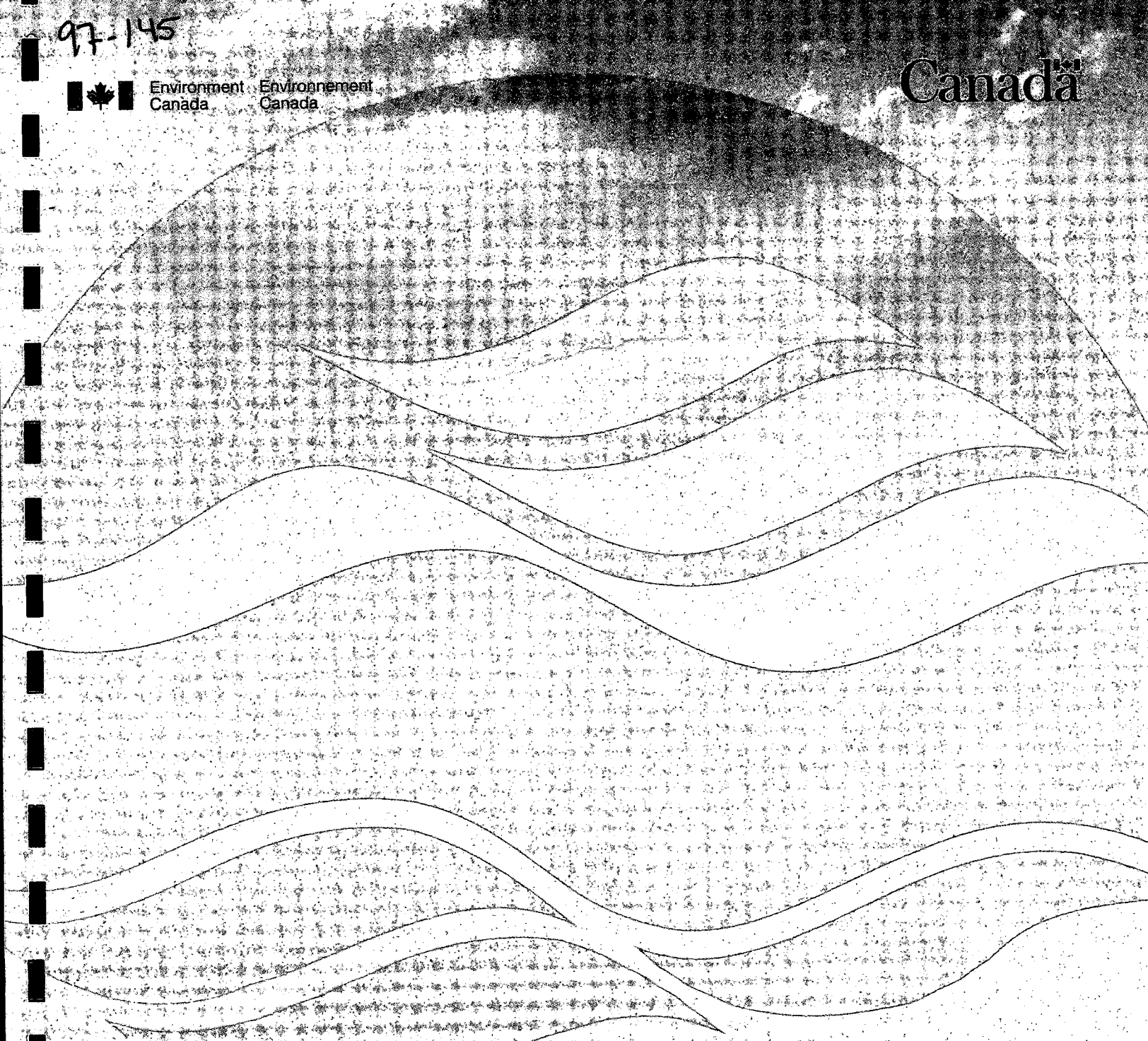

The Interpretation of a Tracer Experiment Conducted In a Single Fracture Under Conditions of Natural Groundwater Flow

BY:

P.A. Lapcevic, K.S. Novakowski

NWRI Contribution No. 97-145

THE INTERPRETATION OF A TRACER EXPERIMENT CONDUCTED IN A SINGLE FRACTURE UNDER CONDITIONS OF NATURAL GROUNDWATER FLOW

by

P. A. LAPCEVIC,
K. S. NOVAKOWSKI,

NATIONAL WATER RESEARCH INSTITUTE
867 LAKESHORE ROAD
BURLINGTON, ON
CANADA
L7R 4A6
905 336 4597
e-mail: pat.lapcevic@cciw.ca

and

E. A. SUDICKY

DEPT. OF EARTH SCIENCES
UNIVERSITY OF WATERLOO
WATERLOO, ON
N2L 3G1

For submission to:
WATER RESOURCES RESEARCH

October, 1997

MANAGEMENT PERSPECTIVE

Title: The Interpretation of a Tracer Experiment Conducted in a Single Fracture under Conditions of Natural Groundwater Flow

Authors: P.A. Lapcevic, K.S. Novakowski and E.A. Sudicky

NWRI Publication #: 97- 145

Citation: submitted to Water Resources Research

EC Priority/Issue:

This manuscript deals with the interpretation of a tracer experiment conducted at the GWRP field site in Clarkson, ON. The work at the Clarkson site has focused on research into the processes of flow and solute transport in a single fracture in sedimentary rock. This experiment is unique and has given us insight into the complexity of the processes affecting aqueous solute transport in a variable aperture fracture at the field scale. The results of this study are relevant to our understanding of solute transport at numerous contaminated sites situated on fractured rock throughout the Great Lakes Basin and elsewhere?

This works supports EC priorities under COA Stream 1.6 (groundwater) and Stream 1.4 (contaminated sites). Additionally, it supports GWRP deliverables under Toxics Result #3.

Current Status:

The manuscript has been submitted to Water Resources Research and is currently in the review stage.

Next Steps:

Further interpretations of the data set from this tracer experiment will likely be carried out at a later date.

ABSTRACT

The development of conceptual models to describe the hydrogeology of sparsely fractured media requires the characterization of the physical properties of discrete fractures at the field scale. In this study, a tracer experiment conducted in a discrete fracture pervading a shale and limestone formation is interpreted. The experiment was conducted under conditions of natural groundwater flow. To initiate the tracer experiment a small quantity of conservative tracer was injected into the fracture plane at an upgradient borehole. The subsequent migration of tracer was monitored in a 27 borehole array drilled in a 35 x 40 m area. Tracer breakthrough was observed in 7 boreholes at distances ranging from 11 to 41 m from the source borehole. The results showed a tracer plume which spread both longitudinally and transversely in the direction of mean groundwater flow. The field breakthrough curves were interpreted using a finite element transport model formulated for two dimensions which incorporates longitudinal and transverse dispersion, diffusion into the rock matrix, and constant or spatially variable aperture in the plane of the fracture. The initial interpretation was conducted using constant aperture. Simulations conducted using variable aperture were completed without conditioning and using a Monte Carlo format in which spatial correlation and variance in the aperture field were varied. From the results of the interpretation conducted assuming a constant aperture, it was found that the mean tracer aperture was approximately 20 % greater than the mean aperture measured by hydraulic methods. Values of matrix porosity ranging between 1 and 3 %, a constant value of longitudinal dispersivity of 0.1 m and a large range in transverse dispersivity from 0.01-0.22 m was required to simulate the data. Trends of increasing aperture and matrix porosity with distance were observed, suggesting transport followed increasingly tortuous pathways which

occur due to variability in the aperture. Simulations of tracer transport using variable aperture fields showed lateral spreading of the tracer plumes with increasing spatial correlation length and variance in the aperture distribution. Simulations of the two-dimensional tracer plume with aperture distributions having a high variance but low spatial correlation length appear to best approximate the field plume. The trends of increasing aperture and matrix porosity with distance were not observed with the variable aperture simulations. This suggests that other processes such as spatial or temporal variability in hydraulic gradient may be responsible for this observation in the results of the constant-aperture simulations.

INTRODUCTION

Theoretical and experimental studies conducted using both artificial and natural fractures in a variety of rock types at various scales and levels of confining stress have shown that the traditional representation of fractures as smooth parallel plates can sometimes be inadequate in characterizing the flow rate in natural fractures (e.g. Raven and Gale, 1985; Brown, 1987; Tsang and Tsang, 1987; Brown, 1995). The results of these studies have led to the development of conceptual models which incorporate more accuracy in the physical attributes of the fractures such as roughness in the fracture walls, variability in the fracture aperture, and contact of the fracture surfaces. In addition, the transport of aqueous contaminants in fractured rock masses is governed not only by the physical properties of individual fractures but also by the properties of the surrounding rock matrix.

Physical measurements of surface roughness have been obtained from natural fractures at scales from 0.1 m to ~ 1 m (e.g. Brown et al., 1986; Gale, 1987; Gentier and Billaux, 1989; Piggott, 1990; Vickers et al., 1992; Hakami and Larssen, 1996). These measurements have been used to statistically characterize the spatial distribution of fracture aperture and develop conceptual models for flow and transport in single fractures. Results have shown that fracture apertures usually follow either a log-normal distribution (Gale, 1987; Hakami, 1995), or a Gaussian distribution (Piggott, 1990; Brown, 1995; Hakami and Larssen, 1996). In addition, distributions of aperture are often observed to have a large variance which indicates the presence of significant heterogeneity (e.g. Cox and Wang, 1993; Hakami and Larssen, 1996).

Fractures with similar statistical distributions of aperture may have very different flow properties due to the spatial relationship of the aperture variations. Fracture surfaces have been determined to be correlated spatially with the degree of correlation related to the scale of

measurement. For example, Vickers et al. (1992) studied surface roughness of a single fracture in a block of welded tuff (0.15 x 0.40 m) and found the aperture variations to be spatially correlated at two scales, one on the order of millimetres and the other on the order of tens of centimetres. In addition, Vickers et al. (1992) found that apertures increased consistently along the entire length of the fracture suggesting that another spatial correlation is observed at a scale well in excess of the sample dimensions. Abelin et al. (1994) determined from aperture measurements spaced 0.01 m apart over a 2 m sample, spatial correlation lengths ranging between 0.05 m and 0.8 m.

It is also well recognized that the regions in which the fracture surfaces are in contact and closed to water flow will strongly influence flow and transport (eg. Pyrak-Nolte et al., 1987).The results of several experimental and numerical studies indicate that smooth fractures will display many small areas of contact with complex topology resulting in an irregular distribution of fluid flow among many small channels. In contrast, rough fractures display fewer, larger contact areas with a smoother topology that concentrates flow in a few large channels (eg. Brown and Scholz, 1985; Brown, 1987; Zimmerman et al., 1992; Piggott and Elsworth, 1992; Odling, 1994). Tortuosity factors determined through comparisons of measured hydraulic apertures to physical apertures have been determined to be a good approximation to account for closure (eg. Piggott and Elsworth, 1993).

Due to the paucity of data at length scales greater than 1.0 m, it is unclear as to whether comprehensive conceptual models for variable aperture fractures, based on laboratory scale studies, (eg. Brown, 1995) can be used to accommodate the full range in physical scale of natural fractures from micron sized cracks to faults. Consequently, to verify such models, data are necessary at scales in the tens to hundreds of metres. Because it is likely impossible to collect point measurements of aperture and wall roughness in sufficient quantity to characterize the spatial distribution at this scale,

other methods of inferring this data must be sought.

Solute transport in fractures at the field scale (10-50 m) has been studied through the use of tracer experiments carried out using one or more boreholes under forced hydraulic gradients. These experiments have been conducted using flow rates that result in groundwater velocities several orders of magnitude higher than that which occur under conditions of natural groundwater flow. Field studies have been conducted in single fractures in crystalline rock (eg. Novakowski et al., 1985; Rasmuson and Neretnieks, 1986; Raven et al., 1988; Abelin et al., 1991a, b; Abelin et al., 1994; Gutiérrez et al., 1997), and in sedimentary rock (eg. Novakowski, 1988; Shapiro and Nicholas, 1989; Novakowski and Lapcevic, 1994). The results of these studies have shown that the interpretation of tracer experiments must account for the mixing in the wellbore and diffusion from the fractures into the unfractured rock matrix in addition to advective and dispersive processes within the fractures. While initial estimates of longitudinal dispersivity have been relatively high and tended to increase with distance, this is probably due to apparent dispersion induced by large mixing volumes in test boreholes.

Accounting for variable aperture in the interpretation of tracer experiments conducted at the field scale is limited by the scarcity of field aperture measurements, as aforementioned. Shapiro and Nicholas (1989) compared the use of lognormal and gamma distributions of fracture aperture to describe the spatial variability in fracture aperture in the analysis of radially converging tracer tests conducted in a discrete fracture in dolostone. The gamma distribution was found to provide a better comparison to field breakthrough curves because the lognormal distribution did not reproduce the sharp rising limb of the data. Using stochastic theory for solute transport in a single fracture of variable aperture, the large difference between hydraulic and tracer apertures from 4 different sites

suggested spatial correlation lengths for the variation in log aperture on the order of 1 m for tests at scales in the tens of metres (Gelhar, 1987).

The interpretation of tracer experiments carried out in fractures in igneous and metamorphic rocks have generally not incorporated the effects of diffusion into the matrix (eg. Novakowski et al., 1985; Cliffe et al., 1988; Raven et al., 1988). This has been justified by measured rock porosities which are generally less than 0.5% in igneous and metamorphic rocks (eg. Skagius and Neretnieks, 1986). Nevertheless, Abelin et al. (1991b) found porosities in the order of 1-7% in the rock adjacent to fractures in granite suggesting that the effect of diffusion into the matrix must be considered. In sedimentary rock, matrix porosities may range as large as 30%, thus, the influence of mass transfer from the fracture plane to the surrounding host rock will be significant. Tracer experiments carried out at a scale in the tens of metres suggest that matrix diffusion may be a dominant process in solute transport in fractured rock with matrix porosity less than 5 % (Novakowski and Lapcevic, 1994).

Tracer experiments, at the scale of hundreds to thousands of metres, have been conducted under conditions of natural groundwater flow in unconsolidated aquifers (e.g. Mackay et al., 1986; LeBlanc et al., 1991) and have been invaluable in providing detailed data sets from which the processes of non-reactive and reactive solute transport under controlled conditions can be investigated. Conducting experiments of this type in fractured rock is problematic due to practical constraints such as the cost of installing observation points, initiating a controlled source condition and minimizing well bore volumes so as not to disrupt the natural groundwater flow. Therefore, only forced gradient experiments have been conducted and interpreted in the literature. The tracer experiment which was conducted and interpreted in this study provides a unique data set for investigating solute transport in a single fracture at the field scale.

The purpose of this study was to investigate the influence of the variability of fracture aperture and closure on the spreading of transported solute. A tracer experiment was conducted in a single fracture under conditions of natural groundwater flow. Through the measurement of hydraulic aperture the fracture plane was determined to have a large variance in fracture aperture and a significant percentage of closure. The results of the experiment are interpreted using a two-dimensional numerical model of solute transport which accounts for both longitudinal and transverse dispersion in the fracture plane, diffusion into the rock matrix and either a constant or variable distribution of aperture. The influence of spatially-variable aperture within a rough-walled fracture plane on solute transport at this intermediate field scale (10-40 m) is investigated using a Monte Carlo study in which a tracer experiment is simulated using aperture fields of varying spatial correlation length and distribution variance. Unconditional simulations are undertaken using a conceptual model based on a Gaussian distribution of fracture aperture which is spatially correlated in two dimensions.

METHODS

Tracer Experiment

The tracer experiment was conducted at a field site located west of Toronto, Canada. The upper 20 m of bedrock at the site consists of a weathered fissile gray to reddish gray shale (Upper Ordovician), thinly bedded (< 0.01 m), with numerous soft mud seams and interbeds of white and pink fossiliferous limestone, up to 0.3 m in thickness. Open horizontal fractures generally appear as discrete features and are associated with the sharp contacts between the shale and limestone interbeds. These fractures originate as bedding plane partings which have developed in horizontal orientations due to stress relief from erosional unloading or isostatic rebound. In this study, a single, extensive horizontal fracture located at approximately 10.5 m below ground surface, is investigated.

The field site is instrumented with 27 boreholes, each 17-18.5 m in depth and 76 mm in diameter, all located within an area approximately 35 m x 42 m in dimensions (Figure 1). The boreholes were completed as open wells and cased through the 3-m of overburden into the bedrock. Both single borehole and multi-borehole hydraulic testing methods (ie. constant head injection tests, pumping and pulse interference tests) were used to determine the distribution of hydraulic aperture ($2b_H$) and interwell connectivity in the fracture (Lapcevic and Novakowski, 1993).

Measured hydraulic apertures in all 27 boreholes indicate a highly-variable distribution ranging from below detection limit (6 μm) to a maximum of 282 μm (Figure 1). The arithmetic mean of the hydraulic apertures (assuming measurements at the detection limit were equal to the detection limit) is 125 μm with a standard deviation of 96 μm. In this relatively shallow horizontal fracture plane, approximately 19 % of the hydraulic aperture measurements are below detection limit and two thirds are over 50 μm.

The average hydraulic gradient within the fracture is approximately 2 x 10^{-3} with groundwater flow to the south-southwest (Figure 2). This mean gradient is based on measurements of hydraulic head using manometers which accessed the isolated fracture in 17 boreholes ($2b_H$ > 50 μm) during the period January to September 1995. During this time period, the hydraulic head within the fracture varied temporally by approximately one metre with the greatest changes occurring during the autumn months and spring snow melt. Measurements of hydraulic head in 4 boreholes during a six week period in the spring of 1995 are shown in Figure 3.

Obtaining reliable estimates of hydraulic gradient within this flat-lying fracture is difficult due to the low value of the hydraulic gradient and the close proximity of the boreholes used to measure the water levels. Differences in hydraulic head on the order of only a few centimetres over tens of metres are observed. Groundwater levels obtained using a water level tape have an accuracy of about ± 0.01 m, and electronic pressure transducers commonly drift substantially over time, thus yielding uncertain results. Assuming that the difference in hydraulic head between boreholes 1 and 26 is representative of the mean hydraulic gradient within the fracture, an estimated hydraulic gradient of 2.4 x 10^{-3} is subject to uncertainty of ± 15 %. For the purpose of interpreting the field results of this study, it was assumed that the hydraulic gradient was both spatially and temporally constant during the tracer experiment.

A schematic of the apparatus used in the source and observation boreholes to conduct the tracer experiment is shown in Figure 4. A sampling packer (Novakowski, 1992) constructed of a neoprene gland over a PVC mandrel with a 0.2 m stainless steel access plate was used to collect samples from the observation boreholes. This system limits the volume in the wellbore to several millilitres while allowing for the direct sampling of the fracture plane intersected by the borehole.

A double packer arrangement was used in the source borehole to isolate a 1.0 m portion of the borehole length. The larger wellbore volume isolated using this system was necessary to ensure mixing of the injected tracer and provide for a sufficiently large source concentration. Mixing of the isolated wellbore zone was accomplished by water circulation using a pump on surface. Pressure transmitters were used in both systems to continuously measure the hydraulic head within the isolated fracture.

The tracer experiment was initiated by injecting a concentrated volume (0.17 L) of fluorescent dye Lissamine FF (1000 mg/L solution) into borehole 1 located in the northeast corner of the site. Lissamine FF has been shown to be a conservative tracer at this site. The tracer injection was followed by a period where previously collected groundwater was injected into the isolated zone (0.12 hr). Injection of water was ceased when sufficient water was injected to achieve the desired source diameter. This method of injection created a 'disc' shaped source of known initial concentration (15 mg/L) centred at the borehole. The disc subsequently migrated down-gradient from the source borehole under conditions of natural groundwater flow after the cessation of injection. The volume of the zone isolated by the double packer system in the source well was 3.3 L. Mixing in this zone was maintained for the duration of the experiment.

Tracer movement was monitored in the fracture plane by extracting groundwater samples using a peristaltic pump at seventeen observation boreholes (those having hydraulic apertures greater than 50 μm). Samples were obtained by first flushing the access line to the packer (1/8" (3.2 mm) I.D. nylon tubing) of 30-40 mL groundwater and then filling a 7 mL polyethylene vial. Samples were analyzed in the field using a Turner Model 112® fluorometer to both monitor tracer movement and to adjust sampling frequency so as to ensure adequate resolution of the breakthrough

curves with minimal disruption to the natural groundwater flow field. Sampling frequency ranged from once an hour to once a day depending on the progress of the tracer plume. Prior to the start of the experiment, background samples were obtained from all boreholes. Additional description of the source condition for the tracer experiment can be found in Novakowski et al. (1995).

Interpretation

The interpretation of the tracer experiment was conducted using a numerical model following two approaches: i) using a representation of the fracture having spatially-constant aperture, and ii) using a representation having variable aperture defined on the basis of spatial correlation length and variance in aperture width. Conditional simulation of the aperture distribution, led to unsatisfactory interpretations of the experimental results. Thus, the influence of a spatially-variable aperture on solute transport in this fracture was investigated used using unconditional simulations only.

Constant Aperture

For the constant-aperture case, the breakthrough curves from the tracer experiment were interpreted using a two-dimensional finite element numerical code for flow (FLOW2D, Frind and Pinder, 1973) and a two-dimensional hybrid finite element code for transport (LTGPLAN, Sudicky, 1990). The flow model was used to estimate the distribution of steady-state groundwater velocity while the transport model was used to simulate conservative solute transport in the discrete fracture.

The transport model is based on the Laplace Transform Galerkin (LTG) technique where the advection-dispersion equation is solved in Laplace space using the Galerkin finite-element method (Sudicky, 1989). A first order approximation is used to describe the solute exchange between the

mobile zone (fracture) and the immobile zone (rock matrix). This is an approximation to the process of matrix diffusion whereby the mass exchange between the two zones is assumed to be linearly proportional to concentration differences between the two regions (Sudicky, 1990). The Laplace-domain concentrations are transformed into real time values outside of the transport code using a robust numerical inversion scheme. The LTG method avoids time stepping by solving for the concentration in Laplace space which is relatively smooth even in areas of widely contrasting velocities (Sudicky and McLaren, 1992). In addition, it has been found that differences in time scale between the rapid advection of contaminants in the fracture versus much slower diffusion into the porous matrix poses less severe numerical difficulties when using the LTG method (Sudicky and McLaren, 1992).

The solution domain was discretized using a rectangular grid (x=35 m and y=42 m) of triangular finite elements having dimensions of 0.5 m in both the x and y directions. The y-axis represents the N-S direction. These dimensions slightly exceed the dimensions of the field site. The source condition for the tracer experiment was simulated using both the flow and transport models in two steps. The flow model was first used to determine the distribution of steady velocity with continuous injection at the source well. These calculated injection velocities were then used in the transport model, and a release of tracer was applied at the source well to determine the spatial distribution of concentration at the end of the finite injection period. The nodal concentrations at the end of the injection period were then used as the initial condition for a subsequent run of the transport code. For the latter run, elemental velocities were calculated under conditions of natural-gradient.

Assuming a uniform fracture aperture, the tracer breakthrough curves at specific observation

wells were simulated by manipulating the aperture, 2b, the longitudinal dispersivity, α_L, the transverse dispersivity, α_T , and the matrix porosity, θ_m, in a systematic fashion. The calculated breakthrough curve at each observation borehole was normalized to the initial source concentration. The input hydraulic gradient (both in magnitude and direction) was specified based on field measurements and was assumed to be constant with time. Transmissivity at each nodal point was determined from the fracture aperture using the cubic law. A value of 1.8×10^{-10} m^2/s was used for the effective molecular diffusion coefficient based on the free water diffusion coefficient for Lissamine FF and a geometric (diffusion tortuosity) factor of 0.4. The geometric factor used in the interpretations of this study is based on a single laboratory experiment conducted using Lissamine FF and Deuterium tracers in a rock core specimen of similar type rock (Novakowski and van der Kamp, 1996). Thus, while variability in the effective molecular diffusion coefficient will influence the values of matrix porosity determined in the type curve interpretations it was assumed to be fixed in the current study.

Variable Aperture

For the simulations conducted using distributions of variable aperture, the aperture fields were generated using a robust random field generator based on the discrete Fourier transform (Robin et al., 1993). In all simulations, an isotropic field with spatial correlation lengths (λ_x,λ_y) equal in the x and y directions, and a exponential covariance model were used to generate two-dimensional aperture fields having a specified mean aperture (<2b>) and variance (σ^2). Boundary effects in the generation process were eliminated by truncating a 256 x 256 array of generated apertures to an array 141 x 169 in size, thus accommodating the existing grid. A grid of finer

dimensions ($\Delta x=\Delta y=0.25$ m) was used for the transport simulations conducted with variable aperture. As before, the steady velocity field was determined for each simulation using the flow model. The source condition for the transport simulations was incorporated in a manner identical to that used for the constant aperture simulations described earlier. Four different correlation lengths for fracture aperture in the plane of the fracture, ranging from 0.5 m to 5.0 m, and three values of aperture variance, ranging from 1000 μm^2 to 10,000 μm^2 were used in this study. In all cases, a mean aperture of 125 μm was used. This mean aperture and range of variance are based on the statistical parameters obtained from the hydraulic aperture measurements collected in the field ($<2b>=126$ μm, $\sigma^2=9800$ μm^2). Negative apertures which were generated when $\sigma^2 = 5000$ μm^2 and 10,000 μm^2, were set to a very small positive aperture (1×10^{-7} μm), thus yielding a truncated Gaussian distribution. The truncation of the Gaussian distributions in this manner creates closure in the aperture field ranging from approximately 5% at $\sigma^2 = 5000$ μm^2 to about 10 % at $\sigma^2 = 10{,}000$ μm^2.

RESULTS

The test conditions and field results for the tracer experiment are summarized in Table 1. During this experiment, Lissamine FF was detected at radial distances ranging from 11 to 41 m in 8 of the 17 observation boreholes (7, 19, 2, 22, 24, 6, 26 and 27) down-gradient from the source borehole. Tracer breakthrough in borehole 2 was not interpretable and thus is not discussed further. Peak concentration ranged over 4 orders of magnitude, between 5 μg/L and 4117 μg/L. Arrival times of the peak concentration ranged from 64 hr (borehole 7) to 269 hr (borehole 26). The duration of the experiment was approximately 1000 hr.

The tracer plume at various times is shown in Figure 5. While the contours of concentration drawn are based on only 17 observation points and thus highly subjective, the results show a plume which is migrating to the southwest and increasing in both longitudinal and transverse directions. It is important to note that the retarding effect of diffusion into the rock matrix is significant. The tailing of the breakthrough curves at individual boreholes indicate that matrix diffusion is responsible for the significant longitudinal spreading of the plume observed in Figure 5. In addition, the field plume shows a decrease in apparent centre of mass concentrations as the migration progresses. For example, after 72 hrs the maximum plume concentration measured 10 m from the source is 3 mg/L, down from an initial source condition of 15 mg/L. In comparison, similar plumes in sand aquifers do not show such decreases in concentration (e.g. Mackay et al., 1986).

Seven tracer breakthrough curves were interpreted assuming aperture to be spatially constant (Table 2). Each field curve was interpreted independently, maintaining a mean hydraulic gradient across the site and a constant direction of groundwater flow (210°N). The flow direction was selected based on the hydraulic head measured in the fracture and the direction of the migration of the tracer plumes (Figures 4 and 6). Uncertainty in determining a mean groundwater flow direction within this fracture arises from the low concentration of boreholes, particularly in the southern portion of the site. Examples of interpreted breakthrough curves are shown in Figures 6 and 7 for the boreholes nearest and farthest from the source. In both cases, the model matches well to all portions of the breakthrough curve. Simulations of the other breakthrough curves show similar results. It was not possible to interpret the breakthrough curve from borehole 24 using the 210°N flow direction. Consequently, a fit obtained using a flow direction of 206°N is included in the table but the resulting parameter values are not included in the averages presented.

Interpretations based on curve-fitting often suffer from non-uniqueness due to the large number of fitting parameters. However, for the present case, different portions of the simulated breakthrough curve were found to be influenced by individual fitting parameters in different ways. For example, fracture aperture influences the position of the peak in time while longitudinal dispersivity influences the shape of the front. Matrix porosity influences the post-peak concentrations (tail) and the magnitude of the peak concentration. For this reason, attempts to obtain alternate matches to the field curves using other possible values for the fitting parameters, were not successful. More discussion of this issue can be found in Lapcevic (1997). To obtain the fits discussed in the following, 2b, α_L, α_T and θ_m were adjusted independently.

The sharp fronts observed in the breakthrough curves at all distances lead to a small longitudinal dispersivity (α_L = 0.10 m). Longitudinal dispersivity does not appear to increase with scale as has been previously observed in other studies (e.g. Raven et al., 1988) and predicted by theoretical arguments (Gelhar et al., 1988). Fitted values of matrix porosity range between 1 and 3 %. Transverse dispersivity values ranged between 0.01 m to 0.22 m.

Table 2 also shows that the aperture (and thus velocity) required to obtain a match increases slightly with distance from the source. This implies that travel paths lengthen with distance as a result of flow through tortuous pathways within the fracture plane. Figure 8a illustrates that at a flow direction of 210°N there is an approximately linear relationship between 2b and distance from the source. Similarly, a slight increase in matrix porosity is also noted with increased distance (~ 1% over 30 m) (Figure 8b).

The presence of tortuous pathways is further corroborated by the large range in transverse dispersivity required to match the generated breakthrough curves to the field data. Higher values

of α_T were required to simulate the breakthrough curves from observation boreholes whose location was not directly down-gradient of the source borehole. For example, borehole 7 which is due south of borehole 1 required a value of α_T=0.14 m while borehole 19 down-gradient required a value of α_T=0.01m. Velocity variations within the fracture leading to transverse dispersion may occur as a result of either variations in fracture aperture, hydraulic transients (ie. temporal or spatial changes in hydraulic gradient) or a combination of both factors.

The ratio of the tracer aperture to hydraulic aperture for individual boreholes ranges from 0.8 to 2.4 (Table 2). Based on this interpretation, the mean aperture determined from the tracer experiment is approximately 25% greater than the mean of the measured hydraulic apertures (i.e. excluding those apertures that are closed) and more than 40% greater than the arithmetic mean of all measured hydraulic apertures. Using only the 7 boreholes in which tracer was detected during the tracer experiment, the mean tracer aperture is about 20 % higher than the mean hydraulic aperture. This means that use of the cubic law and a mean tracer aperture to estimate groundwater velocity, will lead to estimates about a factor of three greater than that using the mean hydraulic aperture. This also illustrates the risk of estimating groundwater velocity based on only one or two hydraulic measurements.

The results suggest the matrix porosity of the host rock is between 1 and 3%. This range is similar to that observed from the results of a forced-gradient tracer experiment conducted previously in the same fracture (Novakowski and Lapcevic, 1994) and is slightly lower than a measurement of 5% determined from a single laboratory diffusion experiment conducted using limestone core from this site (Novakowski and van der Kamp, 1996).

Variable Aperture Simulations

A variogram was constructed from the hydraulic aperture measurements assuming that aperture in this fracture is of an isotropic spatial correlation structure (Figure 9). A total of 347 pairs with 23-65 pairs per lag distance were used to construct this variogram. The small set of data (N=27) and minimal range of lag distances leads to a variogram of poor quality. Nevertheless, the variogram suggests that either fracture aperture in this fracture is spatially uncorrelated or, more likely, that the aperture is spatially correlated at a scale lower than the shortest lag distance. Because the minimum spacing between boreholes is 5.3 m, spatial correlations in aperture variations at scales below 5 m cannot be captured on the basis of the sampling scale. Thus, the results of this geostatistical analysis suggests that the hydraulic apertures cannot be reliably used in conditional simulation of the aperture field in this fracture. It is important to note, however, that the hydraulic aperture measurements do indicate that the distribution of aperture in this fracture is characterized by a high value of variance (ie. ~ 10,000 μm^2).

The potential influence of aperture variability on the tracer experiment was investigated by conducting a Monte Carlo study in which a tracer experiment was simulated using aperture fields with various spatial correlation lengths and variance in distribution. Twenty four realizations of the aperture field were constructed for each set of statistical parameters. The discussion of the results of these simulations is focussed on two forms of output. Firstly, the features of the two-dimensional simulated tracer plumes are discussed and secondly simulated breakthrough curves at points lying approximately along the mean flow direction and at different distances from the source are examined.

A variable aperture field leads to an irregular distribution of groundwater velocities within

the fracture. Aperture distributions with identical statistical parameters (<2b> and σ^2) yet different spatial correlation lengths (λ_x=λ_y) may exhibit very different spatial patterns of velocities (Figure 10). In addition, the nature of the closed areas and interconnected regions of the aperture field will differ with different values for spatial correlation length. For example, smaller correlation lengths will exhibit tortuous pathways around small regions of closure (Figure 10a) while larger correlation lengths with a similar total area of closure will lead to large regions of the fracture plane which are closed and not available to flow (Figure 10b).

Figure 11 shows examples of single realizations of the simulated tracer plume using input aperture distributions which have the same mean aperture (<2b>=125 μm) but different values of σ^2 and λ_x=λ_y. The plume created by assuming a uniform aperture is shown in Figure 11a. Figure 11b shows a plume with σ^2= 2000 μm^2 and λ_x=λ_y=5.0 m, Figure 11c, σ^2=10,000 μm^2 and λ_x=λ_y=0.5 m, and Figure 11d, σ^2=10,000 μm^2 λ_x=λ_y=5.0 m. In Figure 11b the variable aperture distribution results in greater spreading of the plume in the lateral direction when compared to the constant aperture plume. In this case the direction of mean flow is unaffected. Aperture distributions with higher variance but low correlation length (Figure 11c) results in a plume in which there is less lateral spreading and several small areas in the heart of the plume that are tracer free (evidenced by white areas within the plume). These areas correspond to zones of closure in the fracture plane. The general shape of the plume in this case, also follows the mean groundwater flow direction. Lastly, a high variance in aperture and high correlation length leads to significant deviation from the mean flow direction, an irregular plume shape and larger tracer-free areas where closure occurs (Figure 11d). It is important to note that the plumes shown in Figure 11b and, in particular, Figure 11c best approximate the shape of the plumes observed during the field experiment (Figure 5). Because the

hydraulic apertures indicate an aperture distribution with high variance and apertures in several boreholes along the pathway of tracer plume in the field are observed to be closed, the snapshot depicted in Figure 11c is more likely to approximate the field case.

Simulated Breakthrough Curves

Using aperture distributions with the statistical parameters leading to the realizations discussed above, tracer breakthrough curves at specific points on the finite-element grid were also examined. Three points on the grid corresponding to the location of boreholes 19, 6 and 27 at the field site (Figure 1) at distances of 12, 24 and 35 m, respectively, from the source were used as observation points for this component of the study.

Figure 12 shows the variability of breakthrough curves between individual realizations at a distance of 24 m from the source for four different sets of aperture parameters. In Figure 12a, it can be seen that a low variance and a low correlation length leads to a fairly narrow distribution of breakthrough curves. For a low variance but higher correlation length, there is increased spreading between realizations (Figure 12b). Use of a high variance but a low correlation length (Figure 12c) leads to diminished spreading between realizations in comparison to Figure 12b. Lastly, for a high correlation length and a high variance, the presence of fast flow pathways in a few of the realizations causes steep breakthrough at early time and a large spread in peak concentration (Figure 12d).

Aperture distributions with high variance and large correlation length produce plumes that do not intersect the observation point for a large number of the realizations. For example, in simulations with distributions having σ^2=5000 μm^2 and $\lambda_x=\lambda_y$= 5.0 m, the tracer plume misses the

observation point at 12 m from the source borehole in 30 % of the realizations. At 35 m from the source 50 % of the realizations miss the observation point.

Simulated ensemble-mean breakthrough curves at the three observation points are shown and compared to simulation results obtained using constant aperture in Figure 13. Each of the ensemble-mean curves represents the average of 24 realizations with identical <2b>, σ^2 and $\lambda_x=\lambda_y$. Fixed values of θ_m=1%, α_T =0.05 m, and α_L=0.10 m were used in all realizations.

A comparison of the ensemble-mean breakthrough curves obtained with the variable aperture to those curves calculated using a constant aperture shows two consistent trends with increasing $\lambda_x=\lambda_y$; 1) decreased peak tracer concentrations, and 2) earlier time-to-peak concentration. For example, at an observation point 12 m from the source, a 10 to 30 % decline in peak concentration is observed as the correlation length increases from 0.5 m to 5.0 m with aperture distributions in which σ^2 = 1000 μm^2 (Figure 13a). Similar declines are observed at points 24 m and 35 m from the source (Figure 13b and 13c). In addition, a decrease in the time-to-peak concentration in comparison to the constant aperture curve is noted at distances of 12 m and 24 m but it is not as evident at 35 m, although the time scale has increased (Figures 13 a-c). For the case where σ^2=10,000 μm^2, the peak concentration dropped ~50-70% at 12 m and approximately the same at 35 m (Figure 13d-f).

In general, the advanced arrival of the peak tracer concentration for the variable aperture case reflects the presence of high aperture pathways while the drop in peak concentration reflects increased transverse and longitudinal spreading due to the variable velocity fields created by the non-uniform distribution of aperture.

While it was postulated that the trends of increasing aperture with distance observed in the

interpretation of the field data using constant aperture was due to the effects of variable aperture, this is not evidenced in Figure 13. To generate a trend in increased 2b and θ_m, an increase in the diminishment in peak concentration and an advance in peak concentration arrival should be observed with distance. Because this is not observed, it is likely that some other process is responsible for the trend in the field data. Mechanisms such as variable matrix porosity, temporal changes in the hydraulic gradient, or anisotropy in the aperture distribution may be factors. For example, the hydraulic gradient was assumed to be constant in time within the study area and over the course of the tracer experiment. Small changes in hydraulic head on the order of centimetres can lead to velocity variations of the same magnitude as that generated by differences in aperture of tens of microns.

The porosity of the rock matrix was also assumed to be constant over the study area. While it can be reasonably postulated that a heterogeneous distribution of matrix porosities would have significant effects on solute transport, little is known of the porosity variations of sedimentary rock in the horizontal direction at the scale of this site. A detailed study of Permian limestone conducted using 10 wells and over 2000 porosity measurements determined mean porosities of 11.6 % with a variance of 15.6-19.9 $\%^2$, thus suggesting that highly variable distributions of matrix porosities in a single rock formation are possible (Kittridge et al., 1990).

CONCLUSIONS

The objective of this study was to interpret a tracer experiment conducted in a single discrete fracture under conditions of natural groundwater flow. The tracer experiment was conducted by introducing a disc of conservative tracer into a single discrete fracture and monitoring the migration of the resulting tracer plume in 17 boreholes within an area 35 x 40 m. Field observations of the tracer plume showed significant transverse dispersion as the width of the plume increased 2-3 times the source diameter. This transverse dispersion is attributed to velocity variations and closure of the fracture surfaces leading to tortuous pathways. Longitudinal spreading and decreases in the plume centre of mass concentration is attributed to solute mass loss by diffusion from the fracture plane to the surrounding porous rock. Existing numerical models assuming a constant velocity and fracture aperture were used to simulate the tracer breakthrough curves obtained from seven observation boreholes.

A constant value of 0.1 m for longitudinal dispersivity was determined from the type-curve matches of the breakthrough curves. This indicates that the data at this scale shows no evidence for increasing longitudinal dispersion as a function of increasing scale as has been postulated and observed in previous studies (e.g. Raven et al., 1988; Gelhar et al., 1992). The large range of values for transverse dispersivity determined suggests that spatial and temporal velocity variations within the fracture resulted in lateral spreading of the 2-D tracer plume away from the mean groundwater flow direction.

The fracture aperture estimates determined from the tracer experiment ranges from 195-235 μm. Using only the hydraulic aperture from the 7 boreholes in which tracer breakthrough curves were interpreted, the mean tracer aperture is about 20% higher than the mean hydraulic aperture. A

range of values of matrix porosity between 1 and 3% was determined. Trends of increasing aperture and matrix porosity are noted at boreholes further from the source suggesting that transport in this fracture followed tortuous pathways which occur due to variable aperture in the fracture plane and the presence of closed areas.

Simulations of tracer transport using variable aperture fields showed significant lateral spreading of the plume for correlation lengths between 0.5 m and 5.0 m and high variance distributions. Simulated plumes that appear to be most similar to the observed tracer plume are constructed for the case when the correlation length is small and variance is high. Monte Carlo simulations of tracer breakthrough at specific locations in the variable aperture distribution showed that the trend to larger aperture with increasing distance interpreted from the constant aperture simulations is not satisfactorily reproduced using this simple conceptual model of variable aperture in the fracture plane. Other possible mechanisms such as variable matrix porosity, temporal changes in the hydraulic gradient, or anisotropy in the aperture distribution may be responsible for this trend. Further simulations are required to resolve this issue. The breakthrough curves simulated using unconditioned aperture distributions are highly variable and illustrate that the use of ensemble-mean curves is questionable in this case.

Incorporating variable aperture into the interpretation and prediction of solute transport in discrete fractures at scales in the tens of metres is limited by a lack of verified conceptual models of fracture aperture at this scale. In this investigation, the collection of hydraulic aperture measurements at inter-borehole scales of less than 5 m would allow for a more realistic geostatistical examination of the correlation structure of the aperture fields. Without a defensible conceptual model for variable aperture it appears that the use of an effective constant aperture to predict velocity

within single fractures at the field scale is appropriate. This study was conducted to investigate variable aperture as a mechanism for the macro-dispersion seen in the field plume, yet changes in the hydraulic gradient either temporally or spatially may also contribute to the dispersion observed transversely. Additionally, while it is clear that matrix diffusion is a dominant process in sedimentary porous rock, little is known about the spatial variability of matrix porosity within rock aquifers. Further examination of the heterogeneity of matrix porosity will lead to a better understanding of the uncertainty in measuring solute transport parameters caused by not incorporating spatial variability at the field scale. Fortunately, the field data set is unique and of high quality and as such will be amenable to further interpretations. The single fracture examined in this study is conceptually simple and yet the large degree of heterogeneity observed in the aperture field suggests that the degree of field characterization required to make reasonable predictions of flow and solute transport in fractured rock systems will always be substantial to the point of being untenable.

ACKNOWLEDGMENTS

The authors are grateful to J. Voralek, G. Bickerton, C. Flamen, C. Talbot and E. Walker for assistance with the field experiment. Some funding for this study was provided by the Ontario Ministry of Energy and Environment through Grant No. 393G.

REFERENCES

Abelin, H., L. Birgersson, J. Gidlund and I. Neretnicks, A large-scale flow and tracer experiment in granite 1. Experimental design and flow distribution, *Water Resour. Res.*, 27(12), 3107-3117, 1991a.

Abelin, H., L. Birgersson, L. Moreno, H. Widen, T. Agren, and I. Neretnicks, A large-scale flow and tracer experiment in granite 2. Results and interpretation, *Water Resour. Res.*, 27(12), 3119-3135, 1991b.

Abelin, H., L. Birgersson, H. Widen, T. Agren, L. Moreno and I. Neretnicks, Channeling experiments in crystalline fractured rocks, *J. Contam. Hydrol.*, 15, 129-158, 1994.

Brown, S. R. and C. H. Scholz, Closure of random elastic surfaces in contact, *J. Geophys. Res.*, 90(B7), 5531-5545, 1985.

Brown, S. R., A note on the description of surface roughness using fractal dimension, *Geophys. Res. Lett.*, 14(11), 1095-1098, 1987.

Brown, S. R., Simple mathematical model of a rough fracture, *J. Geophys. Res.*, 100(B4), 5941-5952, 1995.

Brown, S. R., R. L. Kranz, and B. P., Bonner, Correlation between the surfaces of natural rock joints, *Geophys. Res. Lett.*, 13(13), 1430-1433, 1986.

Cliffe, K. A., D. Gilling, N. L. Jefferies and T. R. Lineham, An experimental study of flow and transport in fractured slate, *J. Contam. Hydrol.*, 13, 73-90, 1993.

Cox, B. L., and J. S. Y. Wang, Single fracture aperture patterns: characterization by slit-island fractal analysis, in Proceedings of International High Level Radioactive Waste Management Conference, Las Vegas, NV, 1993.

Frind, E. O. and G. F. Pinder, Galerkin solution of the inverse problem of aquifer transmissivity, *Water Resour. Res.*, 9(5),1397-1410, 1973.

Gale, J. E., Comparison of coupled fracture deformation and fluid flow models with direct measurements of fracture pore structure and stress-flow properties, in 28th U. S. Symposium on Rock Mechanics, pp. 1213-1222, A.A. Balkema, Rotterdam, The Netherlands, 1987.

García Gutiérrez, M. E., Guimerà, J., Yllera de Llano, A., Hernández Benitez, Humm J., and Saltink, M., Tracer test at El Berrocal site, *J. Contam. Hydrol.*, 26, 179-188, 1997.

Gelhar, L. W., Applications of stochastic models to solute transport in fractured rocks, SKB Technical Report 87-05, Swedish Nuclear Fuel and Waste Management Co., 55 pp., 1987.

Gelhar, L. W., Welty, C. and Rehfeldt, K. R., A critical review of data on field-scale dispersion in aquifers, *Water Resour. Res., 28(7)*, 1955-1974, 1992.

Gentier, S., and D. Billaux, Caracterisation en laboratoire de l 'espace fissural d'une fracture, in Proceedings of the International Symposium on Rock at Great Depth, vol. 1, pp 425-431, A. A. Balkema, Rotterdam, 1989.

Gustafsson, E. and Klockars, C-E., Studies on groundwater transport in fractured crystalline rock under controlled conditions using nonradioactive tracers, SKB Technical Report 81-07, Swedish Nuclear Fuel and Waste Manangement Co., 58 pp., 1981.

Hakami, E., Aperture distribution of rock fractures, Ph.D. thesis, Dept. of Civil and Environmental Engineering, Royal Institute of Technology, Stockholm, 1995.

Hakami, E., and Larsson, E., Aperture measurements and flow experiments on a single natural fracture, *Int. J. Rock Mech. Min. Sci. & Geomech. Abs.*, 33(4), 395-404, 1996.

Kittridge M. G., Lake, L. W., Lucia F. J. and G. E. Fogg, Outcrop/subsurface comparisons of heterogeneity in the San Andres formation, SPE Formation Evaluation, September 1990, pp 233-240, 1990.

LeBlanc, D. R., S. P. Garabedian, K. M. Hess, L. W. Gelhar, R. D. Quadri, K. G. Stollenwerk and W. W. Wood, Large-scale natural gradient tracer test in sand and gravel, Cape Cod, Massachusetts, 1. Experimental design and observed tracer movement, *Water Resour. Res.*, 27(5), 895-910, 1991.

Lapcevic, P. A. and K. S. Novakowski, Measuring groundwater velocity and hydrodynamic dispersion in a single fracture in fractured shale, Final Report: Ministry of the Environment Grant No. 393G, 259pp., 1993.

Lapcevic, P.A., Tracer experiments conducted in a discrete horizontal fracture under conditions of forced hydraulic gradient and natural groundwater flow, MSc. Thesis, University of Waterloo, Waterloo, ON, 98 pp., 1997.

Mackay, D. M., D. L. Freyburg, P. V. Roberts and J. A. Cherry, A natural gradient experiment on solute transport in a sand aquifer, 1, Approach and overview of plume movement, *Water Resour. Res.*, 22(13), 2017-2029, 1986.

Novakowski, K.S., G. V. Evans, D.A. Lever, and K.G. Raven, A field example of measuring hydrodynamic dispersion in a single fracture, *Water Resour. Res.*, 21(8), 1165-1174, 1985.

Novakowski K. S., Comparison of fracture aperture widths determined from hydraulic measurements and tracer experiments, In Proc: 4th Canadian/American Conference on Hydrogeology, Ed: B. Hitchon and S. Bachu, Nat. Water Well Assoc., Dublin, Ohio, pp.68-80, 1988.

Novakowski, K. S., The analysis of tracer experiments conducted in divergent radial flow fields, *Water Resour. Res.*, 28(12), 3215-3225, 1992.

Novakowski, K.S. and P.A. Lapcevic, Field measurement of radial solute transport in fractured

rock, *Water Resour. Res.*, 30(1), 37-44, 1994.

Novakowski, K. S., P.A. Lapcevic, J.Voralek, and G. Bickerton, Preliminary interpretation of tracer experiments conducted in a discrete rock fracture under conditions of natural flow, *Geophys. Res. Lett.*, 22(11), 1417-1420, 1995.

Novakowski, K. S., and G. van der Kamp, The radial diffusion method 2. A semianalytical model for the determination of effective diffusion coefficients, porosity, and adsorption, *Water Resour. Res.*, 32(6), 1823-1830, 1996.

Odling, N.E., Natural rock profiles, fractal dimensions and joint roughness coefficients, *Rock Mech. Rock Engng.*, 27(3), 135-153, 1994.

Piggott, A. R., Analytical and experimental studies of rock fracture hydraulics, Ph.D. thesis, Pennsylvania State Univ., University Park, Pa., 1990.

Piggott, A. R., and D. Elsworth, Analytical models for flow through obstructed domains, *J. Geophys. Res.*, 97(B2), 2085-2093, 1992.

Piggott, A. R., and D. Elsworth, Laboratory assessment of the equivalent apertures of a rock fracture, *Geophys. Res. Lett.*, 20(13), 1387-1390, 1993.

Pyak-Nolte, L.J., L.M. Myer, N.G.W Cook and P.A. Witherspoon, Hydraulic and mechanical

properties of natural fractures in low permeability rock, *Proceedings of the 6th International Congress on Rock Mechanics*, 1, 225-231, A.A. Balkema, Rotterdam, 1987.

Rasmuson, A., and I. Neretnieks, Radionuclide transport in fast channels in crystalline rock, *Water Resour. Res.*, 22(8), 1247-1256, 1986.

Raven, K. G. and J. E. Gale, Water flow in a natural rock fracture as a function of stress and sample size, *Int. J. Rock Mech. Min. Sci. & Geomech. Abstr.*, 22(4), 251-261, 1985.

Raven, K. G., K. S. Novakowski, and P.A. Lapcevic, Interpretation of field tracer tests of a single fracture using a transient solute storage model, *Water Resour. Res.*, 24(12), 2019-2032, 1988.

Robin, M. J. L., A. L. Gutjahr, E. A. Sudicky and J. L Wilson, Cross-correlated random field generation with the direct Fourier transform method,*Water Resour. Res.*, 29(7), 2385-2397, 1993.

Shapiro, A.M. and J. R. Nicholas, Assessing the validity of the channel model of fracture aperture under field conditions, *Water Resour. Res.*, Vol. 25, No. 5, pp. 817-828, 1989.

Skagius, K. and I. Neretnieks, Porosities and diffusivities of some nonsorbing species in crystalline rocks,*Water Resour. Res.*, 22(3), 389-398, 1986.

Sudicky, E. A., The Laplace transform galerkin technique: a time-continuous finite element theory and application to mass transport in groundwater, *Water Resour. Res.*, 25(8), 1833- 1846, 1989.

Sudicky, E. A., The Laplace transform Galerkin technique for efficient time-continuous solution of solute transport in double-porosity media, *Geoderma*, 46, 209-232, 1990.

Sudicky, E. A. and R. G. McLaren, The Laplace transform Galerkin technique for large-scale simulation of mass transport in discretely-fractured porous formations, *Water Resour. Res.*, 28(2), 499-514, 1992.

Tsang Y. W. and C.F. Tsang Channel model of flow through fractured media, *Water Resour. Res.*, 23(3), 467-479, 1987.

Vickers, B. C., S. P. Neuman, M. J. Sully, and D. D. Evans, Reconstruction and geostatistical analysis of multiscale fracture apertures in a large block of welded tuff, *Geophys. Res. Lett.*, 19(10), 1029-1032, 1992.

Zimmerman, R. W., Chen, D.-W. and Cook, N. G. W., The effect of contact area on the permeability of fractures, *J. Hydrol.*, 139, 79-96, 1992.

LIST OF FIGURES

LIST OF TABLES

TABLE 1. Summary of test conditions and field results for tracer experiment.

Test I.D.	NG5						
Date	17-Aug-94 to 27-Sept-94						
Source Borehole	1						
Observation Borehole	7	19	22	24	6	27	26
Well Radius (m)	0	0.04	0.04	0.04	0.04	0.04	0.04
Hydraulic aperture (μm)	98	248	282	154	85	125	230
Radial Distance (m)	10.8	11.82	15.93	19.12	23.71	34.82	41.23
Tracer Concentration (mg/L)	1000						
Tracer Volume (L)	0.17						
Flushing Volume (L)	3.75						
Injection Time (min)	6.6						
Injection Flow Rate (mL/min)	594						
Peak Concentration (μg/L)*	108	4117	5	64	1307	130	19
Tracer breakthrough (hr) (approximate)	34	36	59	56	50	120	163
Time to peak (hr)	64	71	81	98	130	213	269
Source Concentration (C_o) (mg/L)	15						
Peak C/C_o	0	0.3	0	0	0.1	0	0
Observation Borehole Volume (mL)	0	0	0	0	0	0	0
Injection Borehole Volume (mL)	3335						

*background concentration removed

TABLE 2. Results of field breakthrough curve interpretations using a 210°N direction of mean groundwater flow.

Borehole	Distance from Source (m)	$2b_H$ (μm)	v (m/hr)	2b (μm)	$2b/2b_H$	α_L (m)	α_T (m)	θ_m (%)
7	10.76	98	0.20	195	2.0	0.1	0.14	1.5
19	11.82	248	0.20	195	0.8	0.1	0.01	1.2
22	15.93	282	0.24	215	0.8	0.1	0.13	1.48
24	19.12	154	0.20	200	1.3	0.1	0.22	1.85
6	23.71	85	0.20	200	2.4	0.1	0.15	0.95
27	34.82	125	0.28	235	1.9	0.1	0.02	2.55
26	41.23	221	0.27	230	1.0	0.1	0.08	2.7
Average:		177	0.23	212	1.5		0.09	2.0
Standard Deviation:		77	0.03	16			0.06	0.7

[A]Fit obtained using a flow direction of 206°N. Results for this borehole are not included in average and standard deviation calculations.

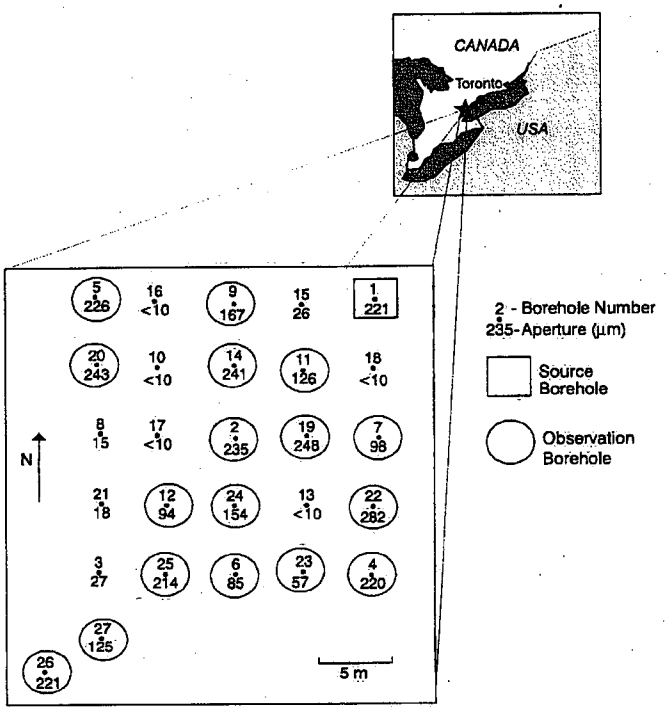

Fig. 1. Location of field site and borehole layout showing hydraulic aperture in each borehole.

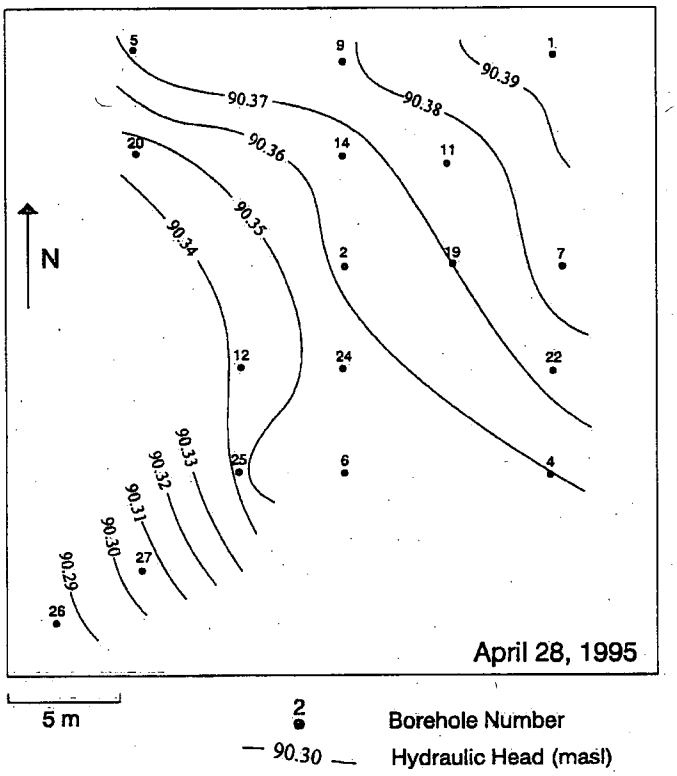

Fig. 2. Contoured hydraulic head in fracture.

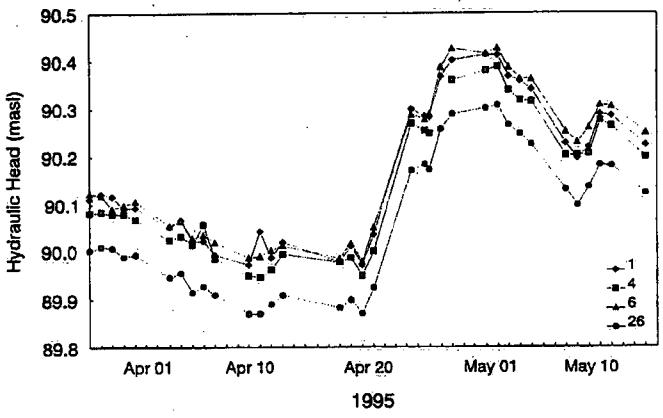

Fig. 3. Hydraulic head measurements in 4 boreholes over a six week period in the spring of 1995.

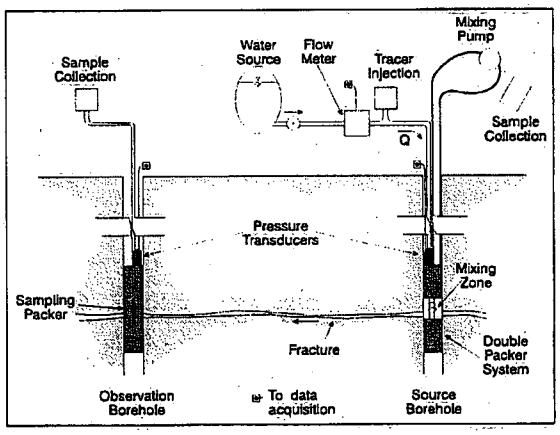

Fig. 4. Schematic of apparatus used to conduct tracer experiment.

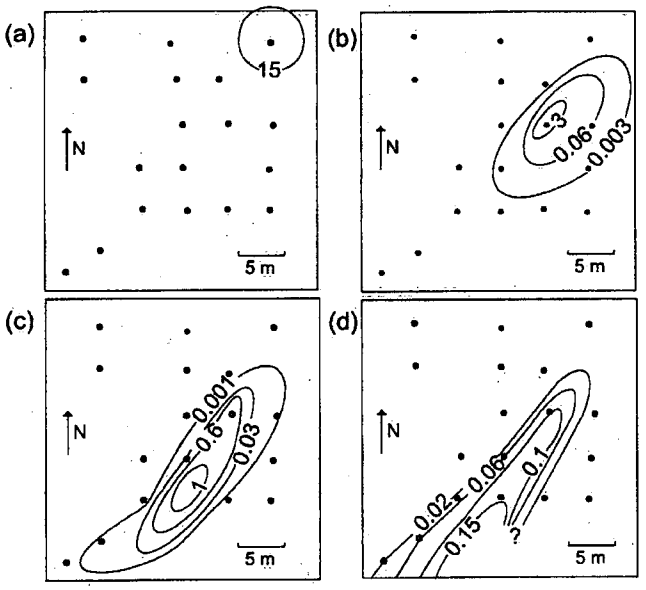

Fig. 5. Field tracer plume at various times: (a) t=0, (b) t=72 hr, (c) t=135 hr, (d) t=276 hr.

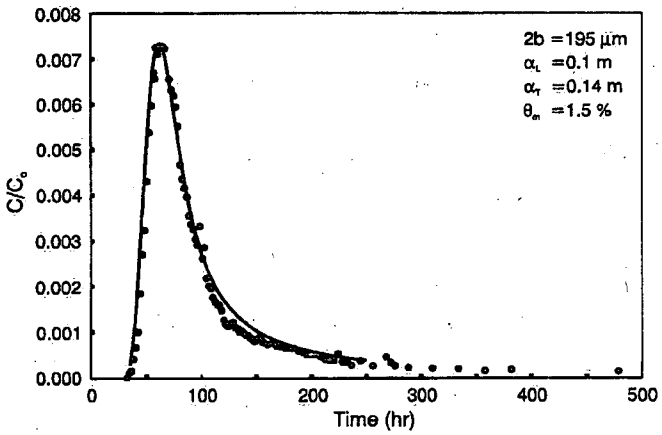

Fig. 6. Type-curve match of tracer breakthrough curve to numerical model in borehole 19 (12 m from source).

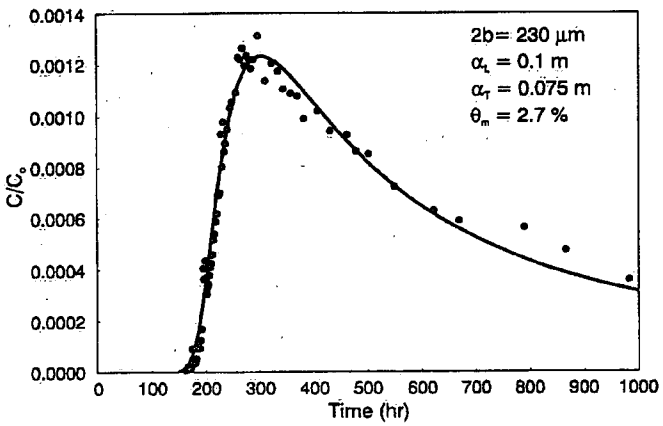

Fig. 7. Type-curve match of tracer breakthrough curve to numerical model in borehole 26 (35 m from source).

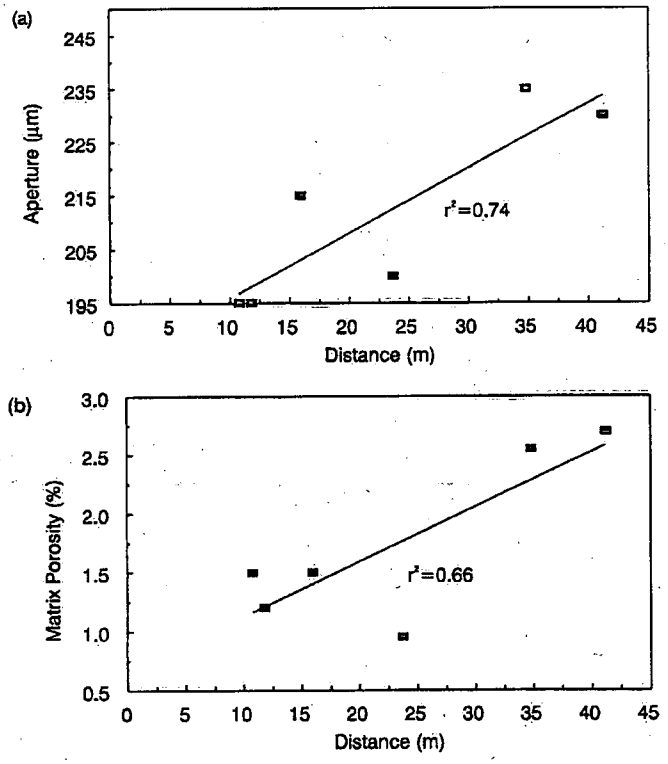

Fig. 8. Variation of determined transport parameter with distance: (a) aperture and (b) matrix porosity.

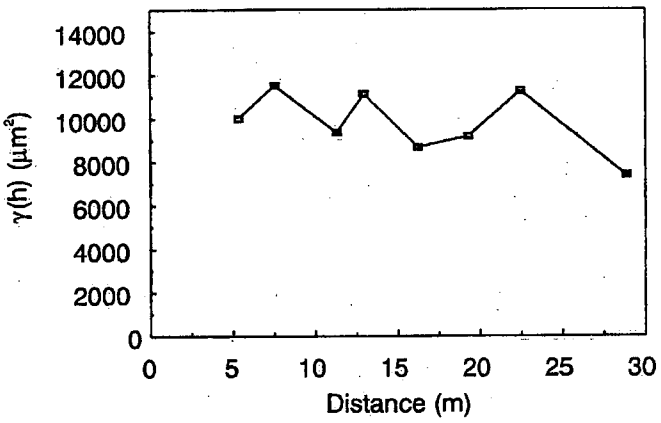

Fig. 9. Variogram of hydraulic apertures.

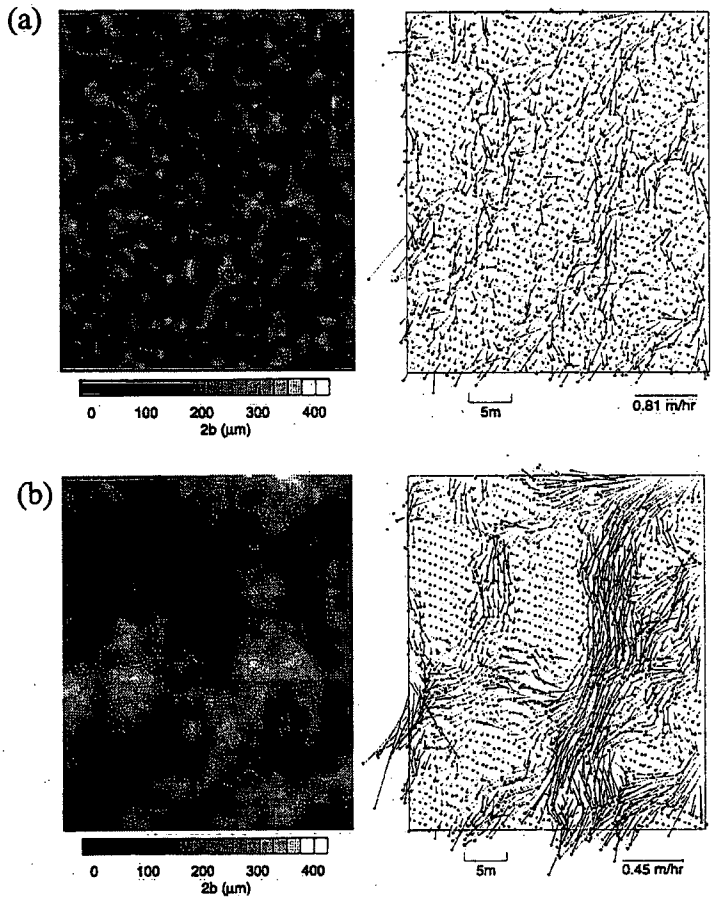

Fig. 10. Examples of generated aperture fields and the resulting distribution of velocities using $\langle 2b \rangle = 125$ μm and $\sigma^2 = 10{,}000$ μm^2: (a) $\lambda_x = \lambda_y = 0.5$ m, (b) $\lambda_x = \lambda_y = 5.0$ m.

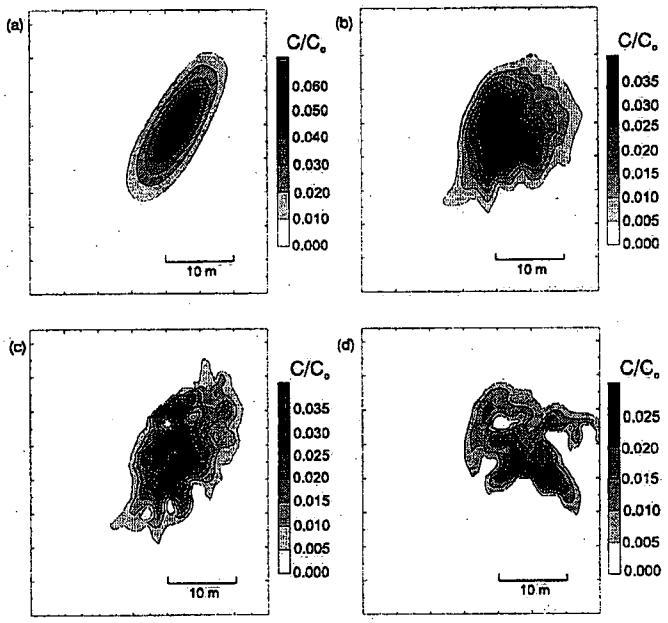

Fig. 11. Examples of simulated tracer plumes generated using a single realization of variable aperture with <2b>=125μm, α_L=0.10 m, α_T=0.05 and θ_m=1%: (a) constant aperture, (b) σ^2=2,000 μm^2, λ_x=λ_y=5.0 m, (c) σ^2=10,000 μm^2, λ_x=λ_y=0.5 m, (d) σ^2=10,000 μm^2, λ_x=λ_y=5.0 m.

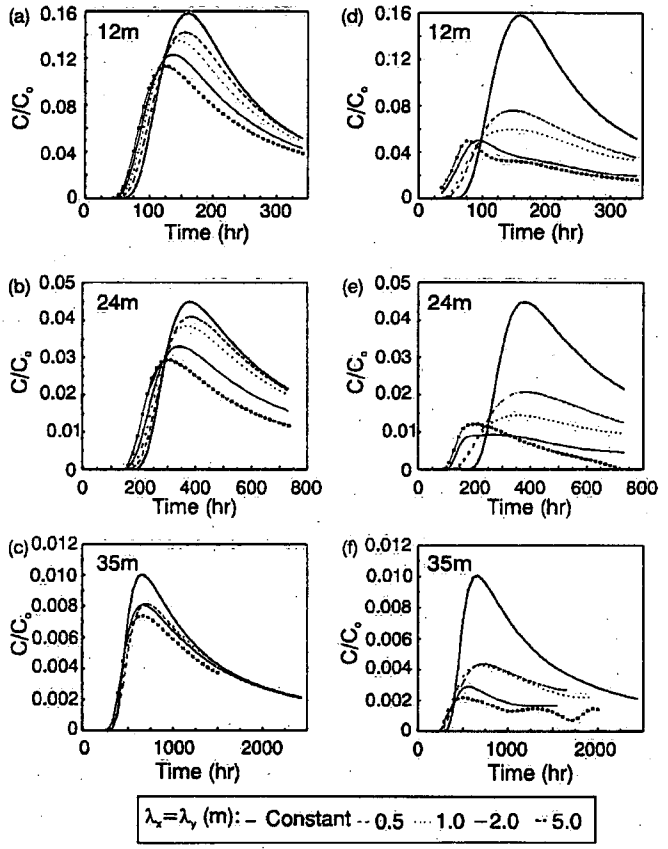

Fig. 13. Average simulated breakthrough curves at three observation points: (a)-(c) σ^2=1000 μm^2 and (d)-(f) σ^2=10,000 μm^2.

PRINTED IN CANADA ON RECYCLED PAPER
IMPRIMÉ AU CANADA SUR DU PAPIER RECYCLÉ

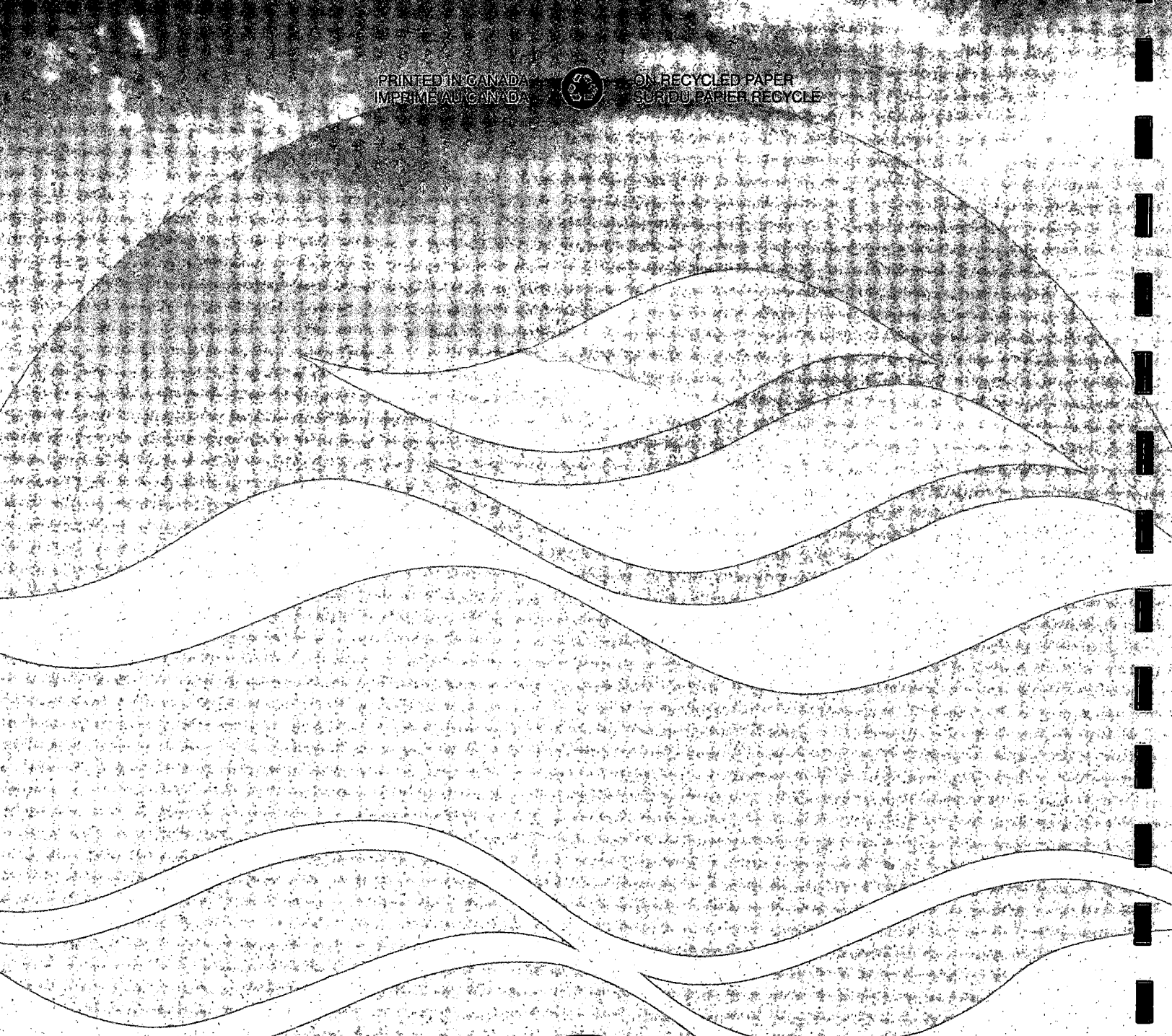

National Water Research Institute
Environment Canada
Canada Centre for Inland Waters
P.O. Box 5050
867 Lakeshore Road
Burlington, Ontario
L7R 4A6 Canada

National Hydrology Research Centre
11 Innovation Boulevard
Saskatoon, Saskatchewan
S7N 3H5 Canada

NATIONAL WATER RESEARCH INSTITUTE
INSTITUT NATIONAL DE RECHERCHE SUR LES EAUX

Institut national de recherche sur les eaux
Environnement Canada
Centre canadien des eaux intérieures
Case postale 5050
867, chemin Lakeshore
Burlington, Ontario
L7R 4A6 Canada

Centre national de recherche en hydrologie
11, boul. Innovation
Saskatoon, Saskatchewan
S7N 3H5 Canada

Environment Canada Environnement Canada

Canada